Hindawi
Wireless Communications and Mobile Computing
Volume 2023, Article ID 6455106, 13 pages
https://doi.org/10.1155/2023/6455106

Research Article

Signal Processing with Machine Learning for Context Awareness in 5G Communication Technology

R. Mohandas,[1] James Luis Alberto Nunez Lira,[2] Walter Edgar Gomez Gonzales,[3] Riyadh A. L. Obaidi,[4] Ibraheem Kasim Ibraheem,[5] Juan Carlos Cotrina-Aliaga,[6] Jana Shafi,[7] K. A. Pranesh,[8] and J. Sam Alaric[9]

[1]*Department of ECE, Balaji Institute of Technology & Science, Warangal, India*
[2]*University Nacional Mayor de San Marcos, Peru*
[3]*Universidad Privada San Juan Bautista, Peru*
[4]*Department of Accounting, Al-Mustaqbal University College, Hillah, Babil, Iraq*
[5]*Department of Computer Engineering Techniques, Al-Rasheed University College, Baghdad, Iraq*
[6]*University Cesar Vallejo, Peru*
[7]*Department of Computer Science, College of Arts and Science, Prince Sattam Bin Abdul Aziz University, Wadi Ad-Dawasir 11991, Saudi Arabia*
[8]*Department of Electrical and Electronics Engineering, Study World College of Engineering, Coimbatore, Tamilnadu, India*
[9]*Department of Electrical and Computer Engineering, College of Engineering and Technology, Wollega University, Nekemte, Ethiopia*

Correspondence should be addressed to J. Sam Alaric; samalaric@gmail.com

Received 6 October 2022; Revised 5 November 2022; Accepted 24 November 2022; Published 30 January 2023

Academic Editor: Anandakumar H

To meet users' expectations for speed and reliability, 5th Generation (5G) networks and other forms of mobile communication of the future will need to be highly efficient, flexible, and nimble. Because of the expected density and complexity of 5G networks, sophisticated network control across all layers is essential. In this context, self-organizing network (SON) is among the essential solutions for managing the next generation of mobile communication networks. Self-optimization, self-configuration, and self-healing (SH) are typical SON functions. This research creates a framework for analyzing SH by exploring the impact of recovery measures taken in precarious stages of health. For this reason, our suggested architecture takes into account both detection and compensating operations. The system is broken down into some faulty states and the "fuzzy c-means" (FCM) approach is used to conduct the classifying. In the compensation process, the network is characterized as the Markov decision model (MDM), and the linear programming (LP) technique is implemented to find the most effective strategy for reaching a goal. Numerical findings acquired from a variety of situations with varying objectives show that the suggested method with optimized operations in the compensation stage exceeds the approach with randomly chosen actions.

1. Introduction

Modern communication enablers and technologies are proliferating; most notably, the fifth generation of wireless and mobile networks has led to an acceleration in the evolution of the Internet of Things designs into intelligent, interconnected ecosystems in recent years (5G). Specifically, the Industrial IoT assumes that widely utilized smart devices, networks, and/or computer components are connected in industrial production settings to achieve very high levels of automation, control, and reliability. This holds for Industry 4.0 as well, also referred to as the fourth industrial

revolution. Examples of such complicated industrial production settings include supply networks for businesses, smart factories, and smart plants (Koursioumpas et al.) [1].

The context-aware 5G network links several devices over the Internet while reducing lag time and providing fast speeds. It employs various kinds of antennas and works on various radio spectrum frequencies. The secondary user will lease the secondary space if the main user is not present. Spectrum leasing and spectrum sensing are the two main techniques for determining if a space is available. A unique kind of mobile network is not brand new, but it differs fundamentally from what is already in existence in many respects. A crucial difference between 4G networks and 5G's specialized radio bands is that 4G networks are utterly worthless. Each of the bands that make up the radio spectrum has unique characteristics. While 5G is anticipated to run at very high frequencies between 30 GHz and 300 GHz, 4G networks now operate at frequencies below 6 GHz. For a variety of reasons, there are numerous high frequencies, but one of the most important is that they can manage a lot of data that happens very quickly (Vijay et al. [2]).

Due to the increased traffic on high-mobility trains, cellular services must be a top priority for every passenger at all times. The deployment of heterogeneous small cells (SC), a key component of context-aware 5G and beyond network densification, is necessary to meet this need. Densifying business support systems (BSs) enhance spectrum efficiency and capacity, which in turn boost the "quality of service" (QoS) but at the expense of the BSs' separate service regions and footprints. However, more BSs with moderate deployments would induce 'frequent handovers' (HOs), up the risk of disconnecting, and rise signaling overhead, which would harm the system's QoS as a whole (Asad et al.) [3]. Figure 1 represents a context-based scheduling scenario for the 5G network.

5G HetNet can satisfy the strict requirements of conventional e-health applications and provide patients with the thorough, individualized treatment they need, thanks to the complementing integration of various radio access technologies (RAT). Furthermore, it provides a variety of benefits including efficient resource usage, improved scalability, and seamless communication. The efficient utilization of 5G HetNets presents a difficulty for context-aware RAT selection due to the diversity of RATs' frequency bands, protocols, and physical and Media access control (MAC) layer multiple access techniques (Priya and Malhotra) [4].

Two essential elements of digital surface model (DSM) designs are interoperability, and interference management since widespread deployment, as projected in 5G, impacts intranetwork and internetwork interference. Dynamic spectrum management that is context aware might be developed by introducing awareness based on context data collection. Mobile devices are now able to choose from a variety of RAT to the 5G technology, which eliminates the limitations of a single RAT by serving as the one global air interface for all currently deployed RAT (Goudar et al.) [5]. We have presented a fuzzy c-means technique to address this problem.

1.1. Contribution. Machine learning for signal processing is the technology that deals with the construction of an effective methodology, FCM, and also makes use of a particular model, MDM, which is capable of identifying and demonstrating a potential underlying pattern in signals, thereby retrieving required data. In 5G network technologies, machine learning has the potential to be a beneficial component for the allocation of resources. For managing intrusions, spectral consumption, multiple paths, network adaptability, many channels of accessibility, and overcrowding, machine learning may be an effective strategy.

2. Related Works

Habbal et al. [6] suggest a ground-breaking "Context-aware Radio Access Technology" (CRAT) selection process that considers network and user characteristics while determining which RAT to provide. A streamlined conceptual paradigm is used to convey contextually aware RAT selection. A mathematical model of CRAT is constructed after taking into consideration the user and network environment, using the "Analytical Hierarchical Process" (AHP) to rank the different RATs and determine the importance of the selection criteria. The suggested CRAT was tested and implemented in the NS3 simulator to make sure it worked as intended. Two scenarios, one set in a shopping mall and the other in a major city, were used to assess the suggested mechanism's potential use in a smart city setting. Using data from handover measurements, typical network latency, throughput, and packet delivery ratio, CRAT was found to be superior to the conventional RAT selection approach, A2A4. To meet the greater bandwidth needs that exist between base-band units (BBUs) and remote radio units (RRUs), large throughput capabilities are required (remote radio units). To meet these criteria, optical fiber is used. This is a significant disadvantage.

Chima et al. [7] refine their approach to scheduling so that it can be used with a full 5G network. Due to the stringent service requirements of the nodes and the connections between them, applications for the industrial Internet of Things are frequently built to run in a distributed manner on the devices and controller computers. For these configurations, 5G will offer the necessary degree of connection and make it possible to host programs, particularly when combined with edge computing. As the Internet of Things device continues to develop and find more widespread use, it becomes more difficult to ensure the confidentiality of the data they collect and communicate. It is really difficult to understand technology. This has issues with connection as well as being power dependent.

Caso et al. [8] created an analysis of research and standardization initiatives, which combines interference control with recommended context-aware interoperability approaches to include network selection, dynamic spectrum management, and resource allocation with context awareness.

Ma et al. [9] add three different areas that deal with these issues. To provide context awareness, the first suggested method is urban event detection, which uses Twitter data to anticipate changes in cellular hotspots. Second, while taking into consideration the projection for skewed-distributed hotspots in metropolitan zones, a proactive 5G load balancing

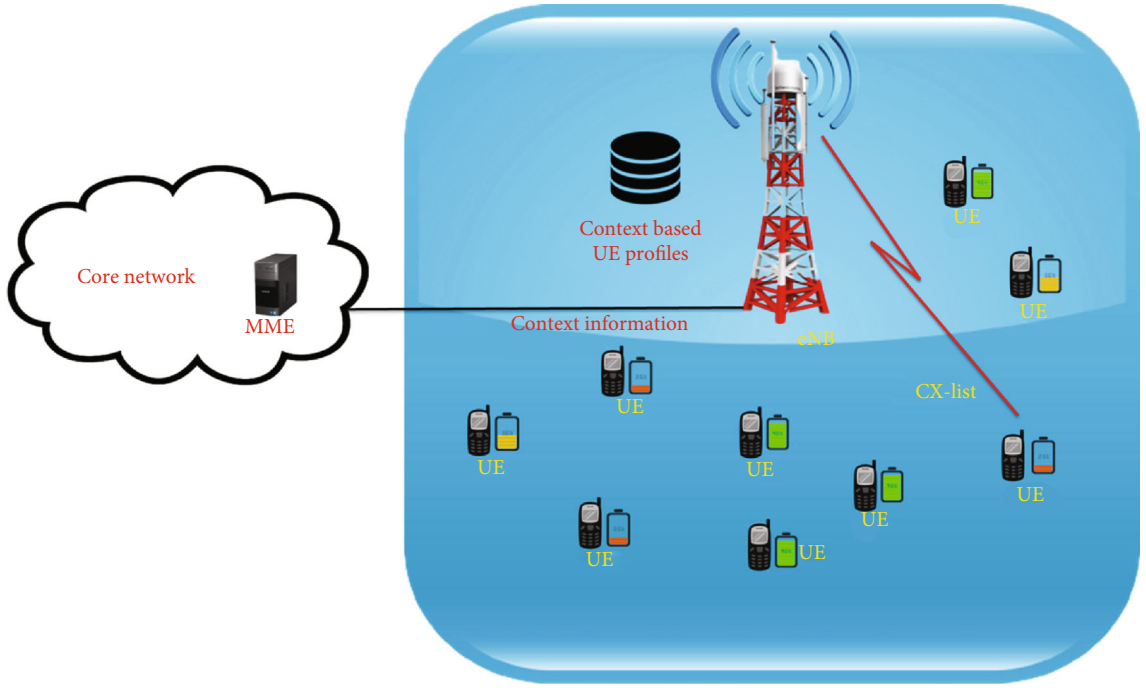

Figure 1: Explored context-based scheduling scenario for the 5G network.

approach is simulated. They eventually improve their proactive, context-aware load-balancing method by forecasting the appropriate activation time. This research is one of the first to incorporate proactive load balancing with actual urban event detection.

Marin et al. [10] allow work offloading to a mobile community-based opportunistic cloud, a novel collaborative paradigm that depends on context awareness, and opportunistic networking is proposed. By putting their technology to work in a practical application, such as preventative patient monitoring, and doing experimental analysis based on actual user traces, they can demonstrate how much energy may be saved while also cutting down on the total time needed to complete tasks. Mobile data offloading is the delivery of data that was initially intended for wireless networks via contrasting connectivity. By carrying more data through the mobile frequencies, offloading frees up capacity for other users.

Sim et al. [11] propose an online learning strategy and handle the millimeter wave vehicular systems beam selection with environmental awareness issues. A multiarmed contextual band problem is exactly how this issue is represented. Next, they suggest fast machine learning (FML), a context-aware online learning method that is lightweight, has assured convergence, and has a demonstrated performance constraint. To learn from and adapt to its surroundings, FML makes use of aggregated incoming data and coarse user location information. They also provide a protocol that complies with industry standards and demonstrates the potential of real-world deployment of FML by making use of the existing cellular network architecture and the forthcoming 5G capabilities.

Ding and Shin [12] explain the context-aware standard-compatible beam update scheme (CarBeam), which allows the base station to decide when to start beam sweeping by utilizing the jittered and quantized layer-1 reference signal received power feedback from the car. CarBeam, in contrast to other studies, exclusively uses the protocols and signals offered by the current 5G beam management system. It may also change its beam-sweeping choices to take into consideration the mobility of moving vehicles for effective beam tracking. The TAPAS Cologne project's vehicle traces are used to assess and demonstrate the efficacy of CarBeam.

Cao et al. [13] integrate context-aware reasoning with cutting-edge augmented reality (AR) apps to provide the most relevant information based on user and environment settings. Computation-intensive AR operations may be delegated to edge servers leveraging 5G networks to provide the best experience possible due to 5G edge computing. They create ConAR, a distributed edge and cloud-based context-aware head-mounted display augmented reality system that uses user-profiles and environmental sensors for navigation. By putting our suggested algorithm for predicting air quality on the edge and in the cloud and connecting to it through 5G and LTE connections, they test the effectiveness of our system. According to our examination of network quality metrics, edge deployment with 5G connectivity performs considerably better than alternative techniques. Our findings demonstrate that 5G edge computing may support context-aware augmented reality (AR) applications that need latency-sensitive analysis. Lack of really accurate spatial positioning systems, a steep and costly training curve, and security issues when AR data is used to impact worker choices are all potential drawbacks.

Piran et al. [14] suggest "Context-Aware Streaming over 5G HetNets (CASH)," which enables them to balance the network context and the content context to reduce network

load and improve QoE. The basic operation of the suggested CASH is a multistep procedure. A single radio controller (SRC), a flow scheduler, and a media server are all part of the integrated architecture offered by CASH. The required user equipment (UE) and the SRC create a metadata file that provides the network context. They evaluate and categorize the contents based on the content context, such as the real bitrate of each scene, using the metadata file they acquired from the SRC in the media preparation server. When the content-context data is introduced, the metadata file is changed. Third, the flow scheduler efficiently controls the flow of content clusters in server-push mode and delivers it to the appropriate RAT based on the bitrate of the content clusters and the bandwidth made accessible by RATs.

Garrido et al. [15] propose a novel technique for training numerous cutting-edge deep neural network (DNN) architectures for traffic forecasting, utilizing domain-specific issue data pertinent to 5G as loss function regularization parameters. Their method, which is independent of the technical domain, is up to 61.3% more accurate than other commonly used loss functions in terms of base station traffic forecasting.

Ge et al. [16] presented that the 5G standard will be expanded to include the installation of user-plane functions (UPFs) by external stakeholders inside the mobile network operator (MNO) network. In light of this, they propose a service function chaining (SFC) architecture for the 5G core network, which would enable MNO to dynamically select the ideal set of UPFs for each flow by those flow's specifics in real time. A testbed network already has the intended architecture. Through practical tests, they show that the UPF deployment technique is a key factor in the final SFC performance and that the performance of their suggested scheme may be quite close to the benchmark. In addition, they provide guidelines for the optimal ways to install UPF in a 5G network.

Islam [17] examines the various caching techniques suggested for 5G networks. There is a discussion of several caching methods that are accessible in the literature. The research also suggests a unique method for context-aware edge caching in 5G networks. In this study, they investigate the caching issue in 5G networks. According to several estimates, cellular networks get 50% of their requests for video content. Given this enormous demand, new techniques are needed in developing 5G networks to handle these rising demands. People have claimed that using a lot of access points may increase capacity in a limited number of studies from the past. Instead, the network densification is constrained. The usage of based stations results in an overabundance of backhaul burden. As a result, current efforts to develop 5G networks fall short of what mobile users demand in terms of high data speeds.

Aschenbrenner et al. [18] suggest a context-aware, location-based approach to manufacturing whereby collaborative robots, in particular, record their constellation, configuration, and adaptation strategy and can adapt to retooling and even relocation modifications. They propose wireless small-cell architecture built on a mobile 5G core network that incorporates location support, a variety of wireless and wired communication technologies, and a smart asset management approach. These mobile nomad cells may function without a complex operator backend on an island and enhance end-to-end connectivity.

Honarvar et al. [19] assess all prospective networks based on the conditions of each subscriber, a global user satisfaction indicator (USI) measures how satisfied users are with their service. The "analytical hierarchical process" (AHP) and utility function theory, which rigorously takes into account both customer- and network-side factors, serve as the theoretical foundation for their strategy. A new method termed opportune context-aware network selection (OCANS) was developed in response to this concept. To choose the ideal network for maximizing user happiness, OCEANS, a network-assisted user-centric method, constantly and automatically considers consumer context.

Adib et al. [6] propose a unique CRAT selection procedure that takes user and network factors into account when deciding which RAT to provide. A streamlined conceptual paradigm is used to convey contextually aware RAT selection. The AHP is then used to balance the weighting of the selection criteria and TOPSIS to rank the various RATs, resulting in a mathematical model of CRAT that takes into account the user and network environment. The NS3 simulation environment was used to implement and validate the recommended CRAT.

Vamvakas et al. [20] introduced an innovative energy control and management architecture that supported licensed and unlicensed spectrum usage to resolve the bandwidth vulnerability that is prevalent in fifth-generation wireless networks. In particular, they examine the principle of charging consumers' authority investments in the unlicensed spectrum as a means of controlling frequency band instability. This is done because they consider the unlicensed band as a common pool of resources (CPR), which has the potential to become depleted if it is used to its full capacity. It raises the risk of being hacked, which harms privacy. In addition, since there is no protection taking place during the setup process, equipment that makes use of 5G technology is an obvious option for hackers or the stealing of information.

3. Proposed Work

The model incorporates both the detection and compensation mechanisms. To discern incorrect states, the detection block processes measured data from the network. The suggested approach uses fuzzy c mean, a machine learning (ML) methodology that falls under the domain of unsupervised learning, to categorize system states into defective, outage, and normal states of operation. To accurately identify the incorrect states, a set of input data with no labels known as a training set will be employed. Table 1 represents a key performance indicator process. The working process of this proposed work is depicted in Figure 2.

An approach is suggested to identify the defective states using a fuzzy c-mean technique based on this context data and key parameter indicator (KPI) statistics. Classifying the current observations into the defective, outage, and

Table 1: Key performance indicator (KPI).

KPI measurements	KPI description
Retainability	The ratio of completed connections to all successfully launched connections.
HOSR	Handover rate of success
RSRP	Reference signal power received
RSRQ	Quality of the reference signal received
SINR	Signal to inference and noise ration
Throughput	A system transmits data at its highest pace.

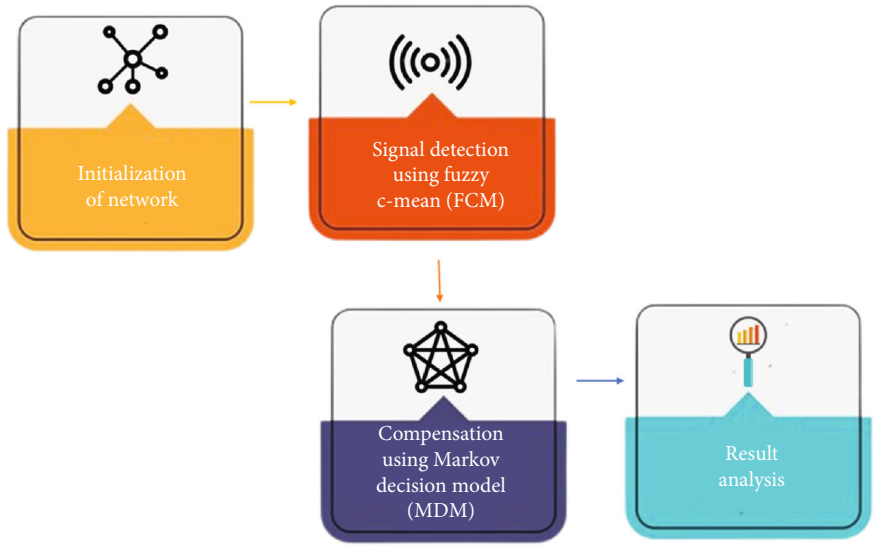

Figure 2: The working process of the proposed work.

normal states is done using a learned random forest that uses training data. As previously said, figuring out which subhealth condition the system is now in is a part of the suggested approach for detection. The aforementioned model is translated into a decision-making formalism for stochastic domains using the Markov decision model (MDM) to decide what actions need to be taken in the following phase to bring the system back to regular operation.

3.1. Fault Detection and Parameters Extraction Model. Determining the cluster centroid points in a collection of unlabeled data using the effective and popular unsupervised clustering technique is known as fuzzy c-means clustering. The only things that need to be produced before the process can start are the training data set and the required number of clusters. The only things needed to use the technique are the training data set and the necessary number of clusters, as indicated by fuzzy c means. Algorithm 1 elaborates the fuzzy c-means clustering.

The overall number of repetitions needed to attain convergence is O (R, K, n), where n is the total amount of input data, R is the total number of repetitions, and fuzzy c is the total set of nodes. The c-means is an effective linear approach because the C and t parameters often have low values. Finding C, the clustering factor, is a significant task. In this study, the elbow technique is used to calculate C. Using a variety of test values for C to fit the model, this strategy aids in choosing the ideal C number of clusters. Each data sample's distance from its centroid point represents the mistake in this instance. The ideal choice for the underlying model's number of clusters is the matching C of the elbow point.

3.2. The Computational Complexity of the FCM Algorithm. The quantity of resources that are needed to execute an algorithm is referred to as either its computational complexity or its simple complexity. Particular attention is paid to the amount of time needed for calculation as well as the need for memory storage.

3.2.1. Process for Compensation. The set of substatuses in the MDM model corresponds to the number of clusters designated by the fuzzy C cluster. A centralized module known as SH-agent handles decision-making in the self-healing (SH) process. The best actions that an operator can take are determined using a quantitative MDM model. Figure 3 shows the model in detail.

There are two sets of logical states and actions in the MDM context. The activities achieve adequate environmental state management to optimize certain targeted performance criteria. The MDM model may be identified by its particular feature of having less memory, where the action

Input: Initial Data set (D), an appropriate amount of clusters (fuzzy).
Create fuzzy cluster centroids from randomly chosen data points (seeds),
While not converged **do.**
Find the nearest data points to each centroid.
To compute, one must assign new centroids while maintaining the existing cluster memberships.
end while.

Algorithm 1: fuzzy c-means algorithm.

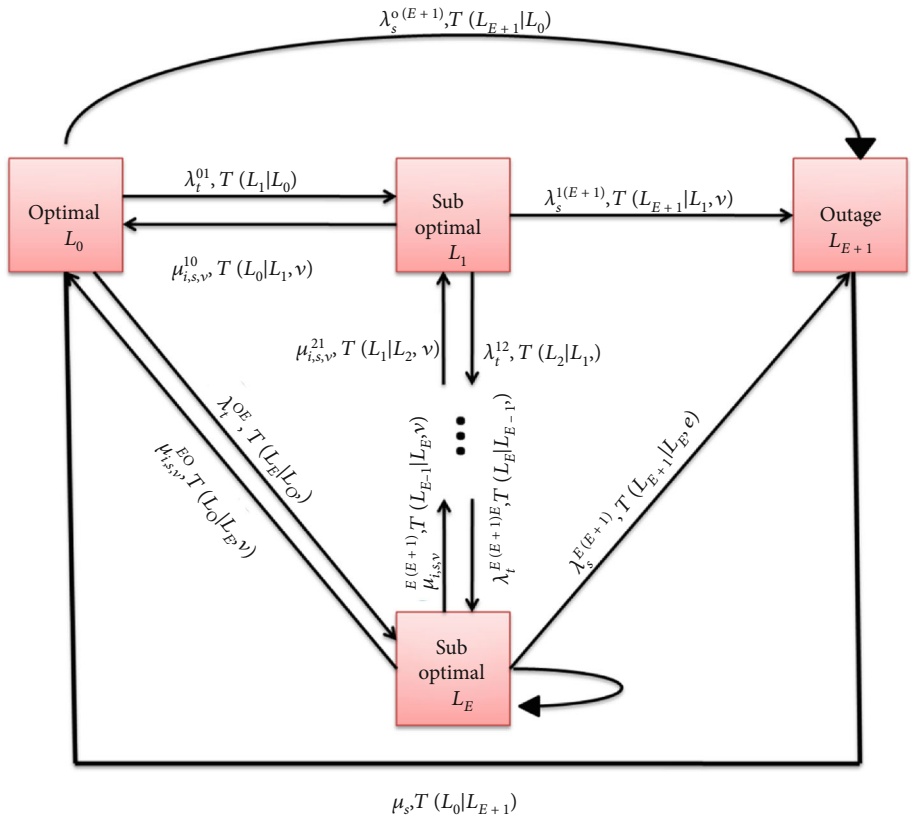

Figure 3: Decision-making based on MDM.

taken at each stage is unrelated to past actions. States, actions, the pace at which states change, and a reward function are these numbers, and they have stated as $(, A, T, r)$. Markov's models are commonly used in the context of mobile cellular networks and SON, and they are primarily used to assess self-optimization (SO) and SH. We suppose that the time is split into intervals of a certain length, T. Thus, a discrete-time MDM (DT-MDM) model is taken into consideration. Thus, we create variable $t = 1, 2 \cdots$ discussing the time-dependent variables, such as states, by reflecting the successive time instants. Let $L(t) \in \mathcal{S} = \{L_0, L_1, .., LE, L_{E+1}\}$ indicate the system condition at the current moment, where $L(t) = L_0$ and $L(t) = L_{E+1}$ depict the ideal and malfunction state, respectively. $\{L_n\}_{n=1}^{E}$ denotes the subhealth statistics. The required performance indicators (PIs) for subhealth statistics depart from their ideal values, but it is presumed that the outage has not yet happened. For the sake of simplicity, we could on occasion disregard it in cases when it would not cause misunderstanding. When the network is subhealthy, it may continue to operate even though the KPIs are dropping below the desired level. The fact that secondary health states $\{L_n\}_{n=1}^{E}$ are arranged in a decaying fashion. $L_1$and L_E correspond to the finest and worse subhealth conditions. According to the concept, a distinct model with various parameter values should be taken into account for each potential defect or failure situation. The first is minor mistakes. The state is driven from its ideal condition by a minor failure, which does not result in a complete outage L_0 to one of the subhealth states $\{L_n\}_{n=1}^{E}$. However, significant faults that result in a complete system failure are taken into consideration, L_{E+1}.The latter occurs either in one of the subhealth levels or in perfect health. It is assumed that the failures are momentary independent. The arrival rates $\lambda_t^{np}$and $\lambda_s^{np}$are from stages n to p, minor and serious failures, respectively (Figure 3), which the Poisson's distribution may be used to represent. When improper behavior is identified frequently

during the subhealth or outage phases, an error/failure recovery module will activate. Let finite set $\mathscr{A} = \{v_1, v_2, \cdots, v_V\}$ with size $|\mathscr{A}| = V$ is the set of every action that is conceivable in each state, $L \in \mathcal{S}$. Here, we maintain the formulation generic by taking probabilistic policies into account. $\pi(v/L)$ is the likelihood of selecting action v in state l; based on a strategy that is optimum $\pi(v/L)$, the recovery module chooses an action $v \in \mathscr{A}$ and works to restore the system to its ideal form after being in a subhealth state. The time it requires for the system to recover from a subhealth status vs. taking action L_n to state L_p is presumable to have an exponential distribution. The time necessary for anomaly detection, diagnosis, and compensation is included in this, with a mean value of $1/\mu_{\mathrm{is},v}^{\mathrm{np}}$. Additionally, it is believed that the compensation period needed to restore an outage to its ideal condition would be exponential with a mean value $1/\mu s$.

Let $T(c'|c,k)$ be the likelihood that states will change into a new state. $c' \in C$ accomplishing action $k \in \mathscr{A}$. The transition matrix T will therefore have the values given in.

$$T = \begin{bmatrix} T\left(l_{0|l_0}\right) & T(l_0|l_0, v_1) & \cdots & T(l_0|l_e, v_e) & T(l_0|l_{e+1}) \\ T\left(l_{1|l_0}\right) & T(l_1|l_1, v_1) & \cdots. & T(l_1|l_e, v_e) & T(l_1|l_{e+1}) \\ T\left(l_{e|l_0}\right) & T(l_e|l_1, v_1) & \cdots & T(l_e|l_e, v_e) & T(l_e|l_{e+1}) \\ T\left(l_{e|l_0}\right) & T(l_{e+1}|l_1, v_1) & & T(l_{e+1}|l_e, v_e) & T(l_{e+1}|l_{e+1}) \end{bmatrix}, \tag{1}$$

where $0 \le T(c'|c,k) \le 1, \forall c, c' \in \mathcal{S} \& \forall k \in \mathscr{A}$ reflects the likelihood that, while the system is in state c, action k will be completed before moving to state c'. Figure 2 and evidence in [1] show that we only take action when a condition is subhealthy $\{c_n\}_{n=1}^{I}$. In other words, recovery measures during a disruption C_{I+1} are not included in the proactive MDM model. Regarding compensation $r(c'|c,k), \forall (c', c) \in \mathcal{S} \& k \in \mathscr{A}$ for particular transitions to c' from c accomplishing, the reward matrix R is denoted in

$$R = \begin{bmatrix} r\left(l_{0|l_0}\right) & r(l_0|l_0, v_1) & \cdots & r(l_0|l_e, v_e) & r(l_0|l_{e+1}) \\ r\left(l_{1|l_0}\right) & r(l_1|l_1, v_1) & \cdots. & r(l_1|l_e, v_e) & r(l_1|l_{e+1}) \\ r\left(l_{e|l_0}\right) & r(l_e|l_1, v_1) & \cdots & r(l_e|l_e, v_e) & r(l_e|l_{e+1}) \\ & r(l_{e+1}|l_1, v_1) & r(l_{e+1}|l_e, v_e) & r(l_{e+1}|l_{e+1}) & \end{bmatrix}. \tag{2}$$

Generally, finding the best insurance is our priority $\pi(v/L)$ which, after a very lengthy series of decisions and acts, adopts that policy and optimizes the predicted return over the long run. The management development program (MDP) directs choices toward maximizing nonzero benefits. Consequently, the method used to determine the rewards $r(L'|L, v)$ establishes the purpose of MDM. The analytical model mentioned above may be utilized to mimic a typical proactive healing process. Any typical hardware or software issues or failure situations may be handled using this SH process. To describe our decision-making in the SH process while taking into account a specific target, part 3 will include creating an analytically tractable MDP. By analyzing the decision-making process, this modeling aims at determining the optimum course of action $\pi(v/L)$. Table 2 denotes a parameter of the MDM model.

To examine its properties in a discrete period, a discretization process is therefore required. Let $F = [f_{\mathrm{np}}]$ represents the element-containing generating matrix f_{np} given by

$$\mathrm{F} = \begin{cases} \text{the transitionrate from } l_n + l_p n \ne p, \\ -\sum_{P=0}^{E+1} f_{\mathrm{np}} n = p. \end{cases} \tag{3}$$

The term "randomization" also applies to this technique. A CTMC's infinitesimal generator matrix Q may be uniformized if it contains finite elements on the main diameter. Fortunately, it will be true that all interesting typical Markov's processes are uniformized. $s = \ln \mathrm{g}_n f_n$, where $F = \sum_{p=0}^{E+1} f_{\mathrm{np}}$. This approach allows for the computation of the transition probability matrix T as

$$T = N + \frac{1}{M} F^T, \tag{4}$$

Here, N is the identity matrix and $\geq s, m \in \mathbb{R}$. With this information in mind, we will formulate the optimization problem in the sections that follow. Consider V to be the expected value of all upcoming rewards, as in

$$M = \lim_{e \longrightarrow \infty} \frac{1}{e} \sum_{t=1}^{e} r_t. \tag{5}$$

r_t is the entire amount of rewards earned up to the current time instant, and $1/e$ applies to guarantee that the value function M is finite. The long-term advantages are minimized by this factor. The objective is to raise V's long-run average reward, as illustrated in [6]. V may be reformulated as follows:

$$M = Jl\{(l)\}, \tag{6}$$

where $r(l)$ represents the reward given to state l. Value function V with relation to a certain policy π, $\mathscr{V}^{\pi}$ is given in

$$M\pi = J_{l,g}\{(l, v)\} = \sum_{l} \sum_{v} r(l, v)\, g(l, v). \tag{7}$$

Here, $0 \le g(L, v) < 1$ is the likelihood of acting in state l and existing in state v. The reward $r(L, v)$ is determined in

$$r(s, a) = \sum_{l} r(l|l, v)\, T(l|l, v).l. \tag{8}$$

Table 2: MDM parameter model.

Parameter	Description
$l(t) \in L$ $L = (L_0 \cdots .., L_{E+1})$	State at time instant t
$V = \{v_1, \cdots \cdots, v_V\}$	A collection of all potential acts
$T(l'\|l, v)$	Probability of a state transition from state l to new state l' when action l is applied
$r(l'\|l, v)$	The potential benefit of changing from state l to a new state l while doing action v
$\pi(v\|l)$	An ideal policy determines the likelihood that action v will be taken at state l.

Consequently, the goal is to establish policies π that maximize $\mathscr{V}^{\pi}$ represented by π^* as given in

$$\pi* = \text{vrm}\pi\text{cax}\sum_{l}\sum_{v} r(l, v)g\,(l, v). \tag{9}$$

On the other side, the likelihood of being in state $L', \forall l \in L$, expressed by $g(L', v)$ is equal to $\sum_v g(L', v) = \sum_{L,v} T(L'|L, v)$ g(L, v). Consequently, we obtain

$$\sum_{v} g(l, v)\, v - \sum_{l,a} T(l|l, v)\, l, v\, g(l, v) = 0 \forall l \in L. \tag{10}$$

It follows that the totality of the probabilities $g(L, v)$ for all values $l \in L$, v ∈ V is equal to 1, which is shown in

$$\sum g(L, v) l, v = 1. \tag{11}$$

Since the likelihood of switching between each metric $(L, L') \in \mathcal{S}$, our MDP model is unichain, hence is not zero. It should be emphasized that if an MDP has just one recurring class and certain transitory stages, it is said to be unichain. The aforementioned issue is of the LP kind, although it should be emphasized that it was solved offline. As a result, the LP problem's computational complexity is immaterial. The likelihood of selecting action v in state l, $\pi(v/L)$ can be calculated as given in Equation (12). Table 3 shows the numerical notations employed in this section.

$$(V|l) = \frac{g(l, v)}{\sum v \epsilon \text{lp}(l, v)}. \tag{12}$$

4. Result and Discussion

A real-world data set is chosen for examination to demonstrate how well the suggested detection/compensation strategy performs. Labeled samples from both healthy and unhealthy conditions are included in this data collection. The number of faulty/subhealth status clusters must be counted as a first step. So, normal state samples are not included in the clustering stage. Three separate incorrect examples are represented in the remaining data; however, the classifier/detector agent is not made aware of this information. For each data point in the data set, SSE within clusters results for a range of C values from 1 to 7 is shown in Figure 4.

Table 3: Numerical notations.

S. no	Notations	Denotation
1	T	Transition matrix
2	R	Reward matrix
3	F	Generating matrix
4	M	Value function

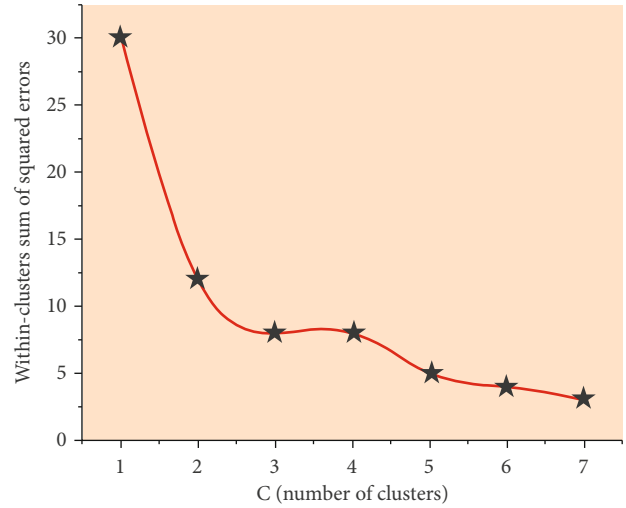

Figure 4: Representation of an optimal number of cluster C.

Using a variety of ML techniques for data mining jobs, the training data set is utilized to locate the clusters and centroid locations using the C-means methodology. Figure 5 shows the clustering results for declaration in terms of the throughput and reference signal received power (RSRP) sample KPIs.

Additionally, Table 4 displays the relationships between the gathered centroid points and 3 clusters in terms of 6 KPIs.

During the compensating stage, a system with three subhealth states, namely, $\{L_1, L2, \text{and}\, L_3\}$ is shown in Figure 2. As a result, l_0 l4 represents the outage and ideal states. We will assume for the sake of simplicity that there is no change in states $L_1$and L_3. We may transfer to states L_1, L_2, L_0, and L_4 from state L_1. It is simple to determine the best course of action for each subhealth condition by extracting the MDP parameters and utilizing the dataset provided in both

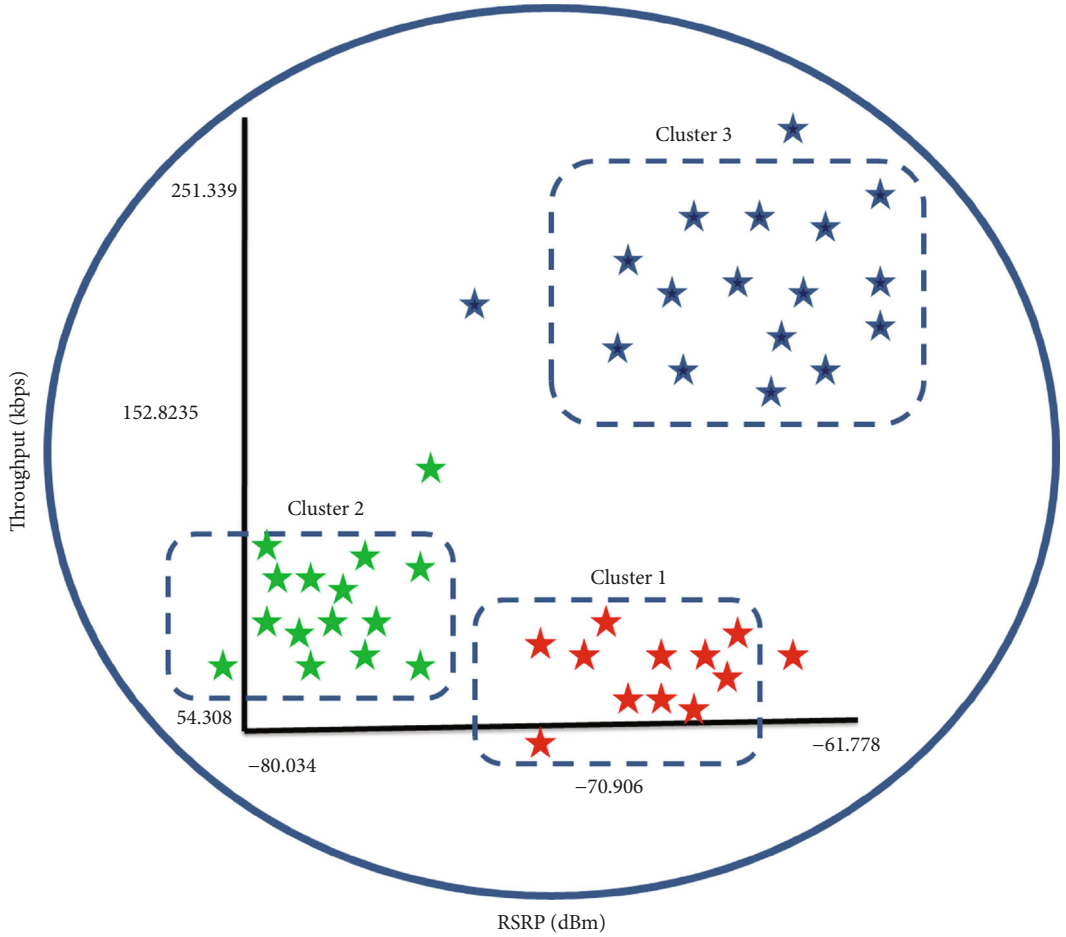

Figure 5: Throughput and RSRP attribute-based fuzzy c-means clustering

Table 4: Centroid points of the cluster.

Attribute	Cluster1	Cluster2	Cluster3
Retainability	0.9951	0.9309	0.944
HOSR	0.9876	0.9229	0.849
RSRP	-77.4961	72.6767	-65.8896
RSRQ	-18.1811	-18.1279	-19.4155
SINR	12.6378	7.0127	13.6656
Throughput	89.1056	68.7371	175.0776

normal and defective states. To make the benefits of the suggested strategy clear in terms of the action policy extraction and compensation process, we examine four scenarios. Table 5 contains each scenario's parameters.

Additionally, as shown in Table 6, the rewards matrix R displays the incentives related to actions v 1 and v 2. The reward values are designed to be nonzero for each of the three subhealth states since we only carry out the activities in subhealth states, and the rewards are exclusively dependent on those actions. The process of transitioning from suboptimal health status to the optimum one is known as recovery and it requires obtaining a reward. Additionally, this is designed to go from one subhealth state to another with a lower score and improved health. Moving from a subhealth stage with a worse status to an outage or another subhealth stage, on the other hand, has a detrimental effect.

In Scenario 1, when action v 1 is completed and the shorter detection compensation time is applied, a bigger reward is given to a certain subhealth condition to aid in its progression to the ideal state. This might reflect a scenario where improving quality of service (QoS) is given precedence over other goals. The second scenario represents the opposite scenario, in which we are more concerned with performance efficiency than recovery time. The system uses less energy to recover in Scenario 2, but it takes a given state a long time to transition to the ideal state. As a result, when action v_2 is chosen, detection compensation time is longer. In instances 1 and 2, $\lambda_s^{n4}(n = 0, 1, 2, 3)$ are both defined as the same. Scenario 3 and Scenario 4's assigned incentives are equivalent to Scenario 1's and Scenario 2's, respectively. However, as seen in Table 4, both situations had increased rates of transition from subhealth stages to outage states. These values were selected from a range of four. This suggests that there is a larger chance of an outage occurring in a worse subhealth condition than there would be in a real-world situation. As shown in Table 4, all other factors are assumed to be the same in all cases.

Table 5: Transition rate.

Parameter	Value
$[\lambda s\,04, \lambda s\,14, \lambda s\,24, \lambda s\,34]$	Scenario 1: $\{\lambda s\,i4\}\ i = 0\,3 = 1/8$ Scenario 2: $\{\lambda s\,i4\}\ i = 0\,3 = 1/8$ Scenario 3: $\{\lambda s\,i4\}\ i = 0\,3 = [1/8, 1/7, 1/6, 1/5]$ Scenario 4: $\{\lambda s\,i4\}\ i = 0\,3 = [1/8, 1/5, 1/3, 1/2]$
λtnp for all possible (n, p)	1/8, for all scenarios
λtnp for all possible (n, p)	6, for all scenarios
μ^{ij}dc, a1 for all possible (n, p)	10, for all scenarios
μ^{ij}dc, a2 for all possible (n, p)	1/12, for all scenarios

Table 6: Rewards assigned in various circumstances.

Parameter	$R \mid v_2$	$R \mid v_1$
Scenario 1 Scenario 3	$\begin{bmatrix} 0.0\,0.1\,0.2\,0.3\,0.0 \\ 0.0\,0.0\,0.1\,0.0\,0.0 \\ 0.0 - 0.1\,0.0\,0.0\,0.1\,0.0 \\ 0.0\,0.0 - 0.1\,0.0\,0.0 \\ 0.0 - 0.3 - 0.2 - 0.1\,0.0 \end{bmatrix}$	$\begin{bmatrix} 0.0\,0.3\,0.4\,0.5\,0.0 \\ 0.0\,0.0\,0.1\,0.0\,0.0 \\ 0.0 - 0.1\,0.0\,0.0\,0.1\,0.0 \\ 0.0\,0.0 - 0.1\,0.0\,0.0 \\ 0.0 - 0.3 - 0.2 - 0.1\,0.0 \end{bmatrix}$
Scenario 2 Scenario 4	$\begin{bmatrix} 0.0\,0.3\,0.4\,0.5\,0.0 \\ 0.0\,0.0\,0.1\,0.0\,0.0 \\ 0.0 - 0.1\,0.0\,0.0\,0.1\,0.0 \\ 0.0 - 0.0 - 0.1\,0.0\,0.0 \\ 0.0 - 0.3 - 0.2 - 0.1\,0.0\,0.0 \end{bmatrix}$	$\begin{bmatrix} 0.0\,0.1\,0.2\,0.3\,0.0 \\ 0.0\,0.0\,0.1\,0.0\,0.0 \\ 0.0 - 0.1\,0.0\,0.0\,0.1\,0.0 \\ 0.0\,0.0 - 0.1\,0.0\,0.0 \\ 0.0 - 0.3 - 0.2 - 0.1\,0.0 \end{bmatrix}$

Figure 6 displays the average rewards obtained for the four scenarios that were taken into account using both optimal and random procedures. The optimum policy yields rewards that are much greater than those of the random approach. However, some crucial insights about the system's behavior and the suggested best-practice approach may be drawn from these findings, which are stated as follows. The system can often recover quickly and avoid entering into an outage as a consequence of the short predicted recovery time. The average payoff is comparable to Scenario 1 for this reason. The scenario is different in Scenario 4.

Due to action v_2 being chosen, the recovery period is lengthy, and in the meantime, there is a greater likelihood that the system would experience severe subhealth conditions (or perhaps an outage). The condition becomes worse when there is an increase in the incidence of $\lambda_s^{\mathrm{np}}$and when subhealth conditions get worse. In comparison to Scenario 2, we can see a considerable drop in attained reward. The median time to recover in the subhealth condition $T_{\mathrm{avg}}^{\mathrm{recovery}}$ is calculated as shown in

$$T_{\mathrm{avg}}^{\mathrm{recovery}} = \sum_{n=1}^{3} g(C_n) \sum_{p=1}^{2} \mu_{\mathrm{is},v_p}^{n0}\, \pi\left(v_p \mid L_n\right). \tag{13}$$

$T_{\mathrm{avg}}^{\mathrm{recovery}}$is the forth situation that was taken into consideration which is shown in Equation (13).The best course of

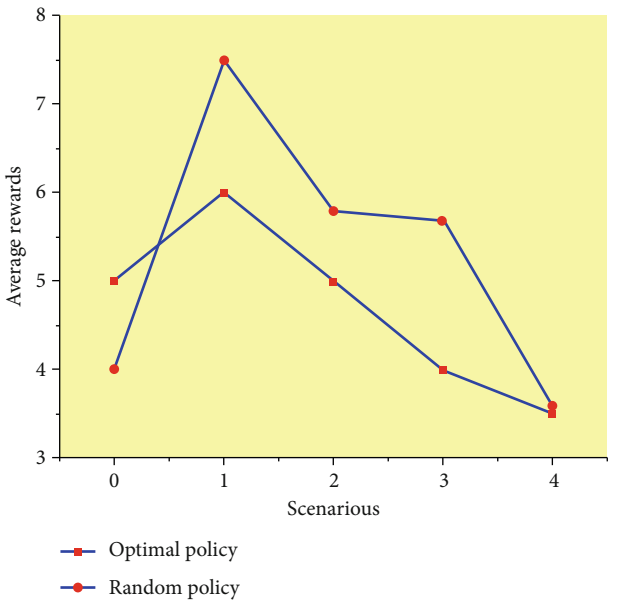

Figure 6: Average benefits obtained by random policy and optimum policy in four situations.

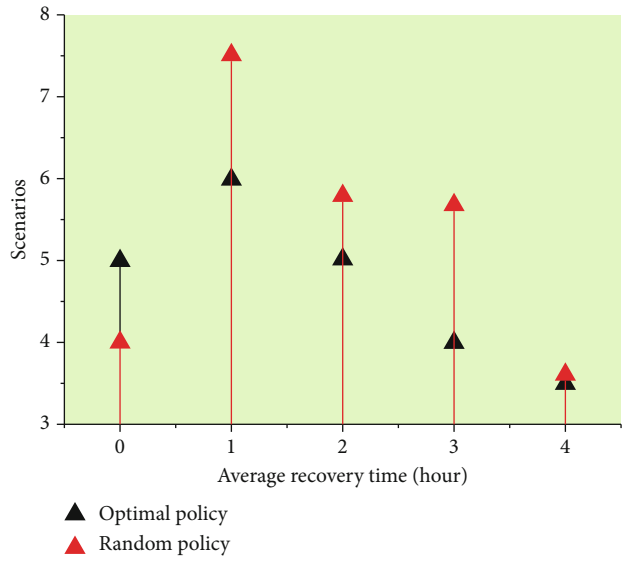

Figure 7: Average recovery time for optimal policy/random policy in four considered scenarios.

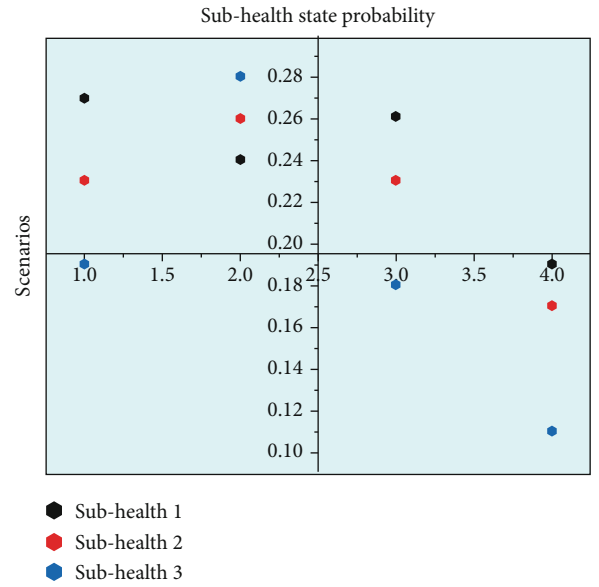

Figure 8: Probability of the subhealth status in 4 scenarios.

action in Scenarios 1 and 3 results in a very quick recovery period. But in Scenarios 2 and 4, we must take action if we want to reap greater benefits v_2 which makes a long recovery time. Therefore, it is entirely expected that the average recovery time for Scenario 2 will increase. However, Scenario 4 needs further explanation. In fact, because of the rise in critical failure λ_s^{np}in the worst subhealth states, practically all effective system recoveries occur in subhealth state 1, then, with a lower probability, but still more frequently than subhealth Condition (2), and finally, subhealth state 3. Consequently, Scenario 2's typical recovery period is quicker. In the four situations taken into account, the average recovery time for the best strategy and the random policy is shown in Figure 7.

When the suggested optimum policy is implemented and the incentives listed in Table 5 are used, in Scenarios 1 through 4, the probability of experiencing subhealth stages is shown in Figure 8. According to Figure 8, the subhealth condition may quickly recover and transition to the ideal state in Scenario 1. Evidently, in scenarios 1 through 3, the likelihood of being in a different state gradually reduces as one moves from state 1 to state 3. Due to scenario 3's higher catastrophic failure rate, this behavior becomes more extreme from λ_s^{14} to λ_s^{34}. A probability of the subhealth condition in 4 situations is shown in Figure 8.

In Scenario 2, the SH agent uses fewer resources while receiving from subhealth states more slowly. The SH agent makes better use of the available resources in this situation; therefore, the recovery time is mostly irrelevant. So, the SH agent could opt to choose the course of action that tends to enhance (or decrease) the possibility that the subhealth state would be the worst and has a longer (or shorter) average recovery time in a particular subhealth condition (or best). Scenarios 2 and 4 perform similarly in terms of the system's propensity to select one of the potential actions. The critical failure rate in Scenario 4 is λ_s^{np}in subhealth 2 is

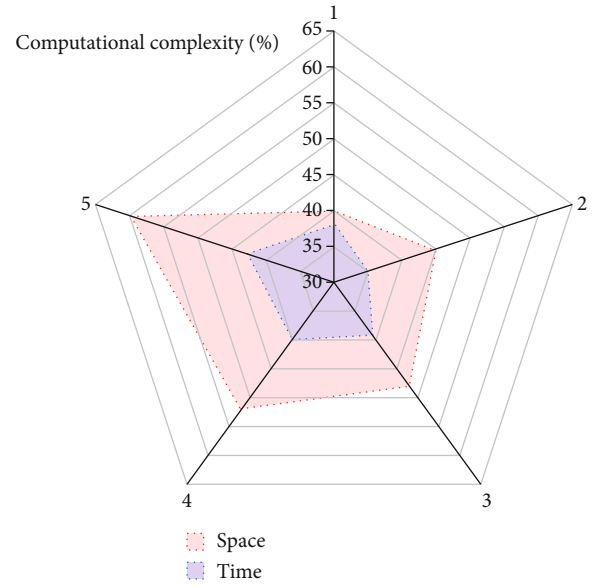

Figure 9: Computational complexity of self-healing.

significantly greater than subhealth 1, and subhealth 3 is significantly greater than subhealth 1 and 2. Since the chance of being in subhealth states drops from subhealth 1 to subhealth 3, it is obvious that the critical-failure rate has a substantial influence.

The amount of space and time that a certain algorithm requires to complete its task is referred to as its computational complexity. Computational complexity is a measure of how complicated an algorithm performs. This is a quantitative investigation of the many ways in which computers could be able to learn information effectively. It is essential to be able to choose algorithms based on their effectiveness and their abilities to solve issues as the challenges themselves

Table 7: Numerical result of computational complexity.

Data set	Computational complexity (%)	
	Space	Time
1	40	38
2	45	35
3	48	39
4	52	40
5	60	43

grow in complexity and scale. It is highly helpful to have the capacity to categorize algorithms according to their level of complexity. Figure 9 displays the computational complexity of the self-healing approach. Table 7 shows the numerical result of computational complexity.

5. Conclusion

Self-healing is the aggressive and independent resolution of connection problems that do not need the participation of individuals. Long-term surveillance and retention of the users must, generally, be used to address legal and moral concerns. Information might also help such methods develop more accurately in regions where certain people frequently reappear. We discussed recent advancements made in the field of context-aware 5G technology and information concerning self-healing solutions. In this paper, we demonstrated a context-aware 5G of the Self-Healing system that uses machine learning methods and has mechanisms for detection and correction. The detection process employed fuzzy c-means clustering with fuzzy parameters with 93% throughput. For the detection procedure, we made use of a real-world data source, and we calculated the total number of subhealth statuses. Four possible scenarios for the compensation phase were also taken into account. To compare our suggested optimum technique with the random action selection policy, we statistically assessed the outcomes for a variety of incentives and performance measures, such as the normal recovery time. The findings demonstrate the merits of the offered analytical model and the superiority of the suggested optimal policies over random action selection policies. Through the prediction of a near-future environment, we developed a strategy to make self-healing proactive. This method should be particularly helpful in small-cell situations in upcoming 5G networks.

Data Availability

All authors confirmed that all necessary data are available in this manuscript.

Conflicts of Interest

The authors declare that they have no conflicts of interest.

References

[1] N. Koursioumpas, S. Barmpounakis, I. Stavrakakis, and N. Alonistioti, "AI-driven, context-aware profiling for 5G and beyond networks," *IEEE Transactions on Network and Service Management.*, vol. 19, no. 2, pp. 1036–1048, 2021.

[2] A. Vijay Vasanth, D. Yuvaraj, P. Janga et al., "Context-aware spectrum sharing and allocation for multiuser-based 5G cellular networks," *Wireless Communications and Mobile Computing*, vol. 2022, Article ID 5309906, 7 pages, 2022.

[3] S. M. Asad, P. V. Klaine, R. N. B. Rais, S. Hussain, Q. H. Abbasi, and M. A. Imran, "Mobility management in the applications of 5G and beyond: a handover skipping topology analysis," in *In 2022 4th Global Power, Energy and Communication Conference (GPECOM)*, pp. 650–654, IEEE, 2022.

[4] B. Priya and J. Malhotra, "5GhNet: an intelligent QoE aware RAT selection framework for 5G-enabled healthcare network," *Journal of Ambient Intelligence and Humanized Computing*, pp. 1–22, 2021.

[5] S. I. Goudar, A. Habbal, and S. Hassan, "Context-aware multi-attribute radio access technology selection for 5G networks," *In Proc. 4th Int. Conf. Internet Appl., Protocols Services (NETAPPS)*, pp. 81–86, 2015.

[6] A. Habbal, S. I. Goudar, and S. Hassan, "A context-aware radio access technology selection mechanism in 5G mobile network for smart city applications," *Journal of Network and Computer Applications*, vol. 135, pp. 97–107, 2019.

[7] M. ChimaOgbuachi, A. Reale, P. Suskovics, and B. Kovács, "Context-aware Kubernetes scheduler for edge-native applications on 5G," *Journal of communications software and systems*, vol. 16, no. 1, pp. 85–94, 2020.

[8] G. Caso, L. De Nardis, and M. G. Di Benedetto, "Toward context-aware dynamic spectrum management for 5G," *IEEE Wireless Communications*, vol. 24, no. 5, pp. 38–43, 2017.

[9] B. Ma, B. Yang, Y. Zhu, and J. Zhang, "Context-aware proactive 5G load balancing and optimization for urban areas," *IEEE Access*, vol. 8, pp. 8405–8417, 2020.

[10] R. C. Marin, R. I. Ciobanu, C. Dobre, C. X. Mavromoustakis, and G. Mastorakis, "A context-aware collaborative model for smartphone energy efficiency over 5G wireless networks," *Computer Networks*, vol. 129, pp. 352–362, 2017.

[11] G. H. Sim, S. Klos, A. Asadi, A. Klein, and M. Hollick, "An online context-aware machine learning algorithm for 5G mmWave vehicular communications," *IEEE/ACM Transactions on Networking*, vol. 26, no. 6, pp. 2487–2500, 2018.

[12] H. Ding and K. G. Shin, "Context-aware beam tracking for 5G mmWave V2I communications," *IEEE Transactions on Mobile Computing.*, p. 1, 2021.

[13] J. Cao, X. Liu, X. Su, S. Tarkoma, and P. Hui, "Context-aware augmented reality with 5G edge," in *In 2021 IEEE Global Communications Conference (GLOBECOM)*, pp. 1–6, IEEE, 2021.

[14] M. J. Piran, S. R. Islam, and D. Y. Suh, "CASH: content-and network-context-aware streaming over 5G HetNets," *IEEE Access*, vol. 6, pp. 46167–46178, 2018.

[15] L. A. Garrido, P. V. Mekikis, A. Dalgkitsis, and C. Verikoukis, "Context-aware traffic prediction: loss function formulation for predicting traffic in 5G networks," in *ICC 2021-IEEE International Conference on Communications*, pp. 1–6, IEEE, 2021.

[16] C. Ge, D. Lake, N. Wang, Y. Rahulan, and R. Tafazolli, "Context-aware service chaining framework for over-the-top applications in 5G networks," in *IEEE INFOCOM 2019-IEEE*

Conference on Computer Communications Workshops (INFOCOM WKSHPS), pp. 50–55, IEEE, 2019.

[17] N. Islam, "A novel context-aware caching scheme for 5G networks," in *In 2019 13th International Conference on Mathematics, Actuarial Science, Computer Science and Statistics (MACS)*, pp. 1–7, IEEE, 2019.

[18] D. Aschenbrenner, M. Scharle, and S. Ludwig, "FlexiCell: 5G location-based context-aware agile manufacturing," *Procedia CIRP*, vol. 107, pp. 1455–1460, 2022.

[19] R. Honarvar, A. Zolghadrasli, and M. Monemi, "Context-oriented performance evaluation of network selection algorithms in 5G heterogeneous networks," *Journal of Network and Computer Applications*, vol. 202, article 103358, 2022.

[20] P. Vamvakas, E. E. Tsiropoulou, and S. Papavassiliou, "On controlling spectrum fragility via resource pricing in 5G wireless networks," *IEEE Networking Letters*, vol. 1, no. 3, pp. 111–115, 2019.